Experimental investigations on the bistable shape states of small air bubbles rising in clean water

Mingming Wu*

Department of Physics, Occidental College, Los Angeles, CA 90041, USA

Morteza Gharib

Graduate Aeronautical Laboratories, California Institute of Technology, Pasadena, CA 91125, USA

(August 3, 2001)

Abstract

This Letter reports experiments on the shape and path of air bubbles (diameter range 0.1 - 0.2 cm) rising in clean water. We find that bubbles in this diameter range have two stable shapes, a sphere and an ellipsoid, depending on the way that bubbles are generated. The spherical bubbles move significantly slower than the ellipsoidal ones of equivalent volume. For bubbles less than about 0.15 cm in diameter, they rise rectilinearly. For larger bubbles, the spherical bubbles follow zigzag paths; while the ellipsoidal bubbles follow spiral paths.

*Corresponding author; electronic mail: mingming@oxy.edu

I. INTRODUCTION

The study of the motion of air bubbles rising in various fluids has been the subject of a large amount of work during the last century (for a review, see Clift, Grace and Weber [1], and a recent review article by Magnaudet and Eames [2]). The problem attracts much attention partly because it is an intrinsically interesting physical problem and it represents an important class of free boundary problem in fluid dynamics [3], and partly because its basic understanding is essential for the study of two phase flows that are of increasing importance in numerous industrial processes. It is known that bubbles of diameter range 0.1 - 0.2 cm rising in clean water are ellipsoidal in shape [1,4]. The bubble path is straight when the equivalent diameter is less than about 0.13 - 0.18, and becomes spiral or zigzag for larger bubbles [5–9,4,10]. Both spiralling and zigzagging bubbles in this diameter regime have been reported [5–9,4,10], however, various experiments are not in agreement whether the bubble spirals or zigzags when the bubble diameter exceeds a threshold. For instance, Saffman [7] and Duineveld [4] observed only zigzagging bubbles using filtered water [7], while Miyagi [5], Aybers & Tapucu [9] observed only spiralling bubbles (water type not specified, in the bubble diameter regime d $<$ 0.2 cm. Among many experimental investigations on bubble motion, few have studied the shape and path of the bubbles simutaneously (Miyagi in 1925, Haberman & Morton in 1953). The current investigation is designed to revisit this intriguing problem further using modern digital imaging systems.

Experimental studies of bubbles rising in water is complicated by its sensitivity to contaminants. It is known that the terminal velocity of the air bubble decreases significantly with the addition of a minute amount of contaminants in water [6,1,11]. This phenomena is especially prominent in the bubble diameter regime of 0.1 - 0.2 cm (see upper and lower solid lines in Fig. 1). Currently, the effect of contamination is best understood by a stagnant-cap model, where the surfactant molecules are swept to the rear of the bubble surface and form a stagnant cap [11]. The rigidity of the stagnant cap elevates the shear stress around the surface of the bubble, and thus results in a reduction of the rising velocity. Experiments

with controlled amount of contaminants have proved the validity of the model. Reported velocity measurements in the literature varies significantly among various expriments (for details, see Fig. 7.3 of Ref.[1]). While some of the spread comes from the experimental errors, the greatest cause is the contamination in water. It should be noted that comparison among different experiments conducted in clean water has been difficult since the criteria for cleanness of water is not well established. Surface tension, as a measure of contaminants, is not sensitive enough for such application. Recent experiments by Duineveld suggests a new method to check whether the rising air bubbles are free of the influence of contaminants [4]. They compared the velocity and shape of bubbles rising in filtered water (18 M$\Omega\cdot$ cm) with theoretical results of Moore, in which the bubble boundary is assumed stress free [4]. A good agreement has been reached as seen in Fig. 1 and Fig. 3.

In this Letter, we report that, in addition to the cleanness of the water, the way that bubbles are generated plays an equally important role in the shape and path of rising air bubbles. Our experimental results show that, in clean water, air bubbles in the previously known ellipsoidal regime (0.1 - 0.2 cm) [1,4] have two stable shapes, a spherical and an ellipsoidal shape, depending on the way that bubbles are generated. The motion of spherical bubbles is shown to be significantly different from that of ellipsoidal ones.

II. EXPERIMENTAL APPARATUS AND PROCEDURE

The main part of the experimental apparatus is the Plexiglas water tank with dimensions of $6'' \times 6'' \times 24''$, which is large enough to neglect the wall effect [6]. At the center of the bottom plate, a specially designed fitting is mounted for the insertion of a glass capillary tube (Clay Adams) or a hypodermic needle. The bubble is released through the capillary tube or the hypodermic needle. The bubble generation method used in our experiments is similar to the one used by Saffman [7] and Duineveld [4]. To differentiate it from other generation methods, we name it a gentle - push method. The bubble generation apparatus consists of a straight capillary, a Teflon L-shape capillary embedded in a three ports valve (Hamilton, HV Plug) and two glass syringes (see Fig. 2). All the components are filled with water

from the water tank except syringe one. Syringe one is used to supply air, it is controlled by a syringe pump (Hamilton, Microlab 501A). The smallest volume that the syringe pump dispenses is 0.1μl. Syringe two (Harvard Apparatus, PHD 2000), on the other hand (See Fig. 2(b)), provides a pressure to force the air bubble through the straight capillary tube. To generate a bubble, a desired volume of air is first released into the L-shape capillary (see Fig. 2(a)) by syringe one. Second, the L-shape capillary is rotated 90^o clockwise to position shown in Fig. 2(b) and the air bubble is gently pushed out by syringe two through the straight capillary into the water tank. It is important that syringe two is operated at a slow rate of 2 μ l/min or less to ensure that bubbles are released into water quasi-statically.

The bubble images are recorded by a high speed camera (1000fps, Kodak Ektapro Motion Analyzer, Model 1000 HRC) together with a 90mm Macro lense. The camera typically takes an image of 512 pixel $\times$384 pixel with a viewing window of 1.84 cm $\times$ 1.38 cm, in which the lower bound is $\sim$ 2.0 cm above the needle tip. The contours of the bubble images are located using Matlab (Mathworks Inc). The long axis a and the short axis b of the bubble are obtained using a Fourier transform method described in Ref. [4] by Duineveld (N=6 is used in our analysis). The diameter of the bubble is calculated using $d = (a^2 b)^{1/3}$. The error for the diameter measurement is $\pm 0.001 cm$.

The bubble trajectories are recorded by a specially designed 3D imaging system, which is mounted on the top of the water tank. The camera maps out the (x, y, z) coordinates of the bubble, where x and y are lateral positions of the bubble, and z is the vertical distance above the needle. Here, z is obtained using a quantitative defocusing mechanism [12]. A typical viewing window of the 3D imaging system is 1.5 cm $\times$ 1.5 cm $\times$ 20 cm, in which the lower bound is at least $\sim$ 20 cm (or $\sim$ 100d, d is the bubble diameter) above the needle tip. The 3D imaging system is designed in such a way that the spatial resolution in the x-y plane is about 40 times better than the resolution along the z direction, making it an ideal instrument for recording trajectories with small lateral movements. In the current setting, the lateral spatial resolution is 0.005 - 0.01 cm and the vertical resolution is 0.02 - 0.4cm, where the resolution varies with the distance between the bubble and the camera.

For the data reported in this paper, we used clean water from a lab in the chemistry department, Occidental College. The water is first taken from a deionized water source of the chemistry building, which has been pretreated by a Culligan water purification system [13]. It is then distilled by an autodistiller (Wheaton split-stream D-10N), and filtered by a 3-module filtration system (Nanopure, Barnstead) in the lab. The surface tension σ of the water is 72.8dyn/cm at 21.8^{o}C measured with a Fisher Scientific tensiometer (Tensiomat Model 21). Experiments are also carried out using water from the chemistry department at Caltech, in which the water is filtered with a 4-module filtration system (Nanopure, Barnstead) with specific resistance of $\gtrsim 18$ MΩ·cm. Experimental results are consistent with the results presented below. Extreme caution is taken to keep the tank as clean as possible. Once the tank is filled with water, it is sealed immediately with plastic sheets. Air filters (VWR Scientific, 0.20 μ m) are installed at the air entrance to the bubble generation mechanism and the two ventilation holes at the top of the water tank. The temperature of the water during the experiment is 22$\pm$0.3^{o}C. To further ensure that our water is clean, we repeated experiments of Duineveld [4] in our experimental setup, good agreements are reached as discussed in the following paragraphs.

III. RESULTS

When a bubble is released into the water tank, both the high speed camera and the 3D imaging system are triggered simultaneously. For a typical experimental run, a sequence of 1000 images are recorded in one second by the high speed camera, in which two of them in the middle of the viewing window will be used for shape and size measurements. The 3D imaging system records a sequence of 60 images in one second, among which only those within the viewing window of the camera (typically more than 45 data points) will be used to obtain the bubble trajectory (x,y,z,t). The vertical velocity of the bubble is extracted from a linear fit to the data (z,t). In Fig. 1, the crosses and circles are velocity curves of bubbles generated by the gentle - push method. The difference between the upper (cross) and lower (circle) curves is the size of the capillary tube from which bubbles detach. The

inner diameter of the capillary tube is $d_i = 0.0267$ cm for upper curve and 0.120 cm for lower curve. To ensure that the lower curve is not caused by contamination in water or in bubble generation apparatus, we intentionally carry out experiments using same batch of water. In Fig. 1, the lower (circle) and the upper (cross) curves are obtained consecutively using the same apparatus and water except for the capillary tubes. The lower curve is obtained first.

Images of bubbles at a position $\sim 2.5cm$ above the capillary tube is recorded with the high speed camera. The aspect ratio χ (long axis a divided by short axis b) versus Weber number We are shown in Fig. 3. Here, Weber number is defined as $We = 2\rho U^2/\sigma$, where ρ is the density of the water. Fig. 3 shows that bubbles generated by the small capillary tube are mostly ellipsoidal in shape, its aspect ratio ranges from 1.1 - 2.2; while the bubbles generated by the large capillary tube are mostly spherical in shape, and its aspect ratio ranges from 1.00-1.08.

We compared the results of our experiments with the experimental results of Duineveld [4] as well as theoretical results of Moore [14]. Duineveld used a similar bubble generation method as the gentle - push method described above, and the inner diameter of their capillary is 0.025 cm. Both velocity curve (U versus d) and the aspect ratio curve (χ versus We) of ellipsoidal bubbles from our experiments agree well with those from Duineveld's experiment (See Fig. 1 and Fig 3). Deviations occur for bubbles larger than $d = 0.18$ cm. This is likely due to the ways that velocities are defined in two experiments. U refers to vertical velocity in our experiment while it is referred to the actual velocity of the bubble in Duineveld's experiment. The agreement with results of Moore is reasonably good at smaller bubble diameter and less so at larger diameters. This may be attributed to the over estimation of bubble deformation in the theory as suggested by Duineveld [4].

To understand effects of the size of capillary on the shape and motion of bubbles, we studied bubble images close to the capillary. Fig. 4 shows time series of images using capillary tubes of two different sizes. For the upper row of images, the capillary size $d_i = 0.0267$ cm, which is much smaller than the size of the bubble. The curvature at the bubble detachment point exhibits a local maximum. Such deformation gives rise to a strong

axisymmetric surface wave, which in turn propels the bubble to a large initial speed. For the lower row of images, the capillary size d_i = 0.120 cm, which is similar to the size of the bubble. The bubble keeps its spherical shape due to the weak perturbations from the detachment process. By analyzing consecutive images in Fig. 4, we obtain a final vertical rising velocity of 18.5 cm/s at t = 20ms for the spherical bubble; while an intermediate speed of 30.0 cm/s is reached at t = 30ms for the ellipsoidal bubble. The final velocity of the ellipsoidal bubble in Fig. 4 is 33.4 cm/s.

The bubble trajectories are shown to be sensitive to the bubble shape. Fig. 5 shows bubble trajectories for spherical and ellipsoidal bubbles of various diameters. For ellipsoidal bubbles, a straight path of the bubble switches to a spiral path (see row (a) and (b) of Fig. 5) when the bubble diameter exceeds $\sim$ 0.15 cm or aspect ratio exceeds $\sim$1.6. For nearly spherical bubbles, the straight path of the bubble switches to a zigzag path (see row (c) and (d) of Fig. 5) when the bubble diameter exceeds $\sim$0.15 cm or Reynolds number exceeds $\sim$ 280. The details of the transitions are being investigated and will be reported in a later publication. Note that the lateral motion of the zigzag path is much smaller than that of spiral path.

We repeated our experiments using a second generation method which is named a pinch - off method. This method has been used frequently in previous investigations [5,6,9,10,15]. For generating a bubble using pinch-off method, air comes from a syringe and goes directly to the hypodermic needle located at the bottom of the tank. The bubble detaches naturally from the needle due to buoyancy force. The bubble size depends on the needle size as well as the shape of the needle tip. For the bubble to detach naturally from the needle, the inner diameter of the needle d_i needs to be much smaller than the bubble diameter d. In our case, d_i ranges from 0.031 - 0.044 cm. The shape and path of the bubbles generated by the pinch - off method are the same as those of bubbles generated by the gentle - push method with capillary d_i = 0.0267cm (See triangle curves in Fig. 1 and Fig. 3 for details).

These experimental results resolve some of the disagreements in the current literature. Saffman used a gentle-push method in which a capillary of inner diameter of 0.16 cm was

used [7], thus only zigzagging bubbles were observed. On the other hand, Miyagi [5] and Aybers & Tapucu [9] used a pinch-off method, thus only spiralling bubbles were observed. Duineveld [4] reported that only zigzagging bubbles were observed. However, they indicate that their bubbles could be spiralling since bubble trajectories were not the primary concern of their investigations [16].

It should be mentioned that our experimental results are consistent with previous findings that bubbles rise at a much slower rate in contaminated water. It is observed in experiments of Fdhila and Duineveld [11] as well as a few tests conducted in our lab that bubbles in the diameter regime of 0.1 - 0.2 cm are always spherical in shape in water saturated with contaminants, regardless of the way that bubbles are generated. Systematic studies of the effects of contaminations on the shape of the bubbles are however still needed.

IV. SUMMARY AND DISCUSSIONS

We find that, in clean water, the shape and path of bubbles in the diameter range of 0.1 - 0.2 cm are sensitive to the size of the capillary tube from which they detach. When releasing to water quasi-statically, bubbles retain ellipsoidal shape when they detach from a small capillary tube; while they retain spherical shape when they detach from a large capillary tube. The ellipsoidal bubbles exhibit a spiralling path instability, while the spherical bubbles exhibit zigzagging path instability when the bubble diameter exceeds $\sim 0.15cm$. In water saturated with contaminants, the shape and path of bubbles are insensitive to the way that bubbles are generated. The bubbles retain spherical shape and always undergo zigzagging path instability. It should be noted that the drag coefficients computed using the velocity curves in Fig. 1 for spehrical bubbles rising in both clean and dirty water are larger than oscillating solid spheres [17]. One intriguing question is - what are the sources of this unusually large drag experienced by spherical bubbles.

Acknowledgement

We would like to thank Professor P. G. Saffman for insightful discussions and encouragement on the subject. We acknowledge undergraduate students Erin Englert, Marin Markov

from Occidental College and Ben Welander from Caltech for their help during experimental work. Wu wishes to thank Frederick Taugwalder who offered generous help during her stay at Caltech. This work is supported by the Office of Naval Research (N00014-98-1-0017), the Petroleum Research Fund (ACS-PRF# 32904-GB9) and the Research Corporation (C-C4612).

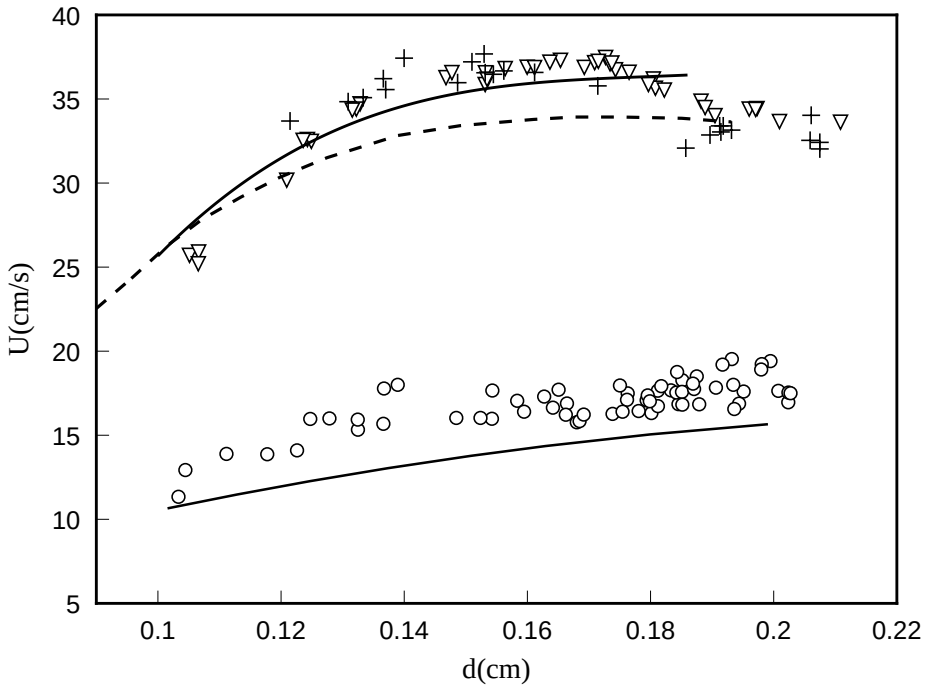

FIG. 1. Vertical terminal velocity U versus diameter d of bubbles generated by a gentle-push method with capillary tube of $d_i = 0.0267$cm +, $d_i = 0.120$ cm ◯, and a pinch-off method ▽. The upper solid line is data taken in clean water by Duineveld[4], the upper dashed line is results from analytical calculation of Moore[14], and the lower solid line is data taken in water saturated with contaminants from Ref. [1].

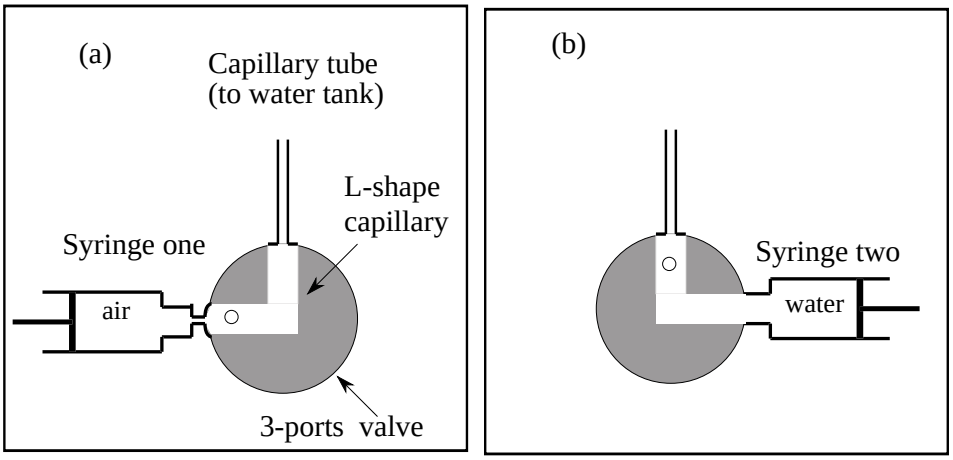

FIG. 2. Schematics for the gentle - push bubble generation method.

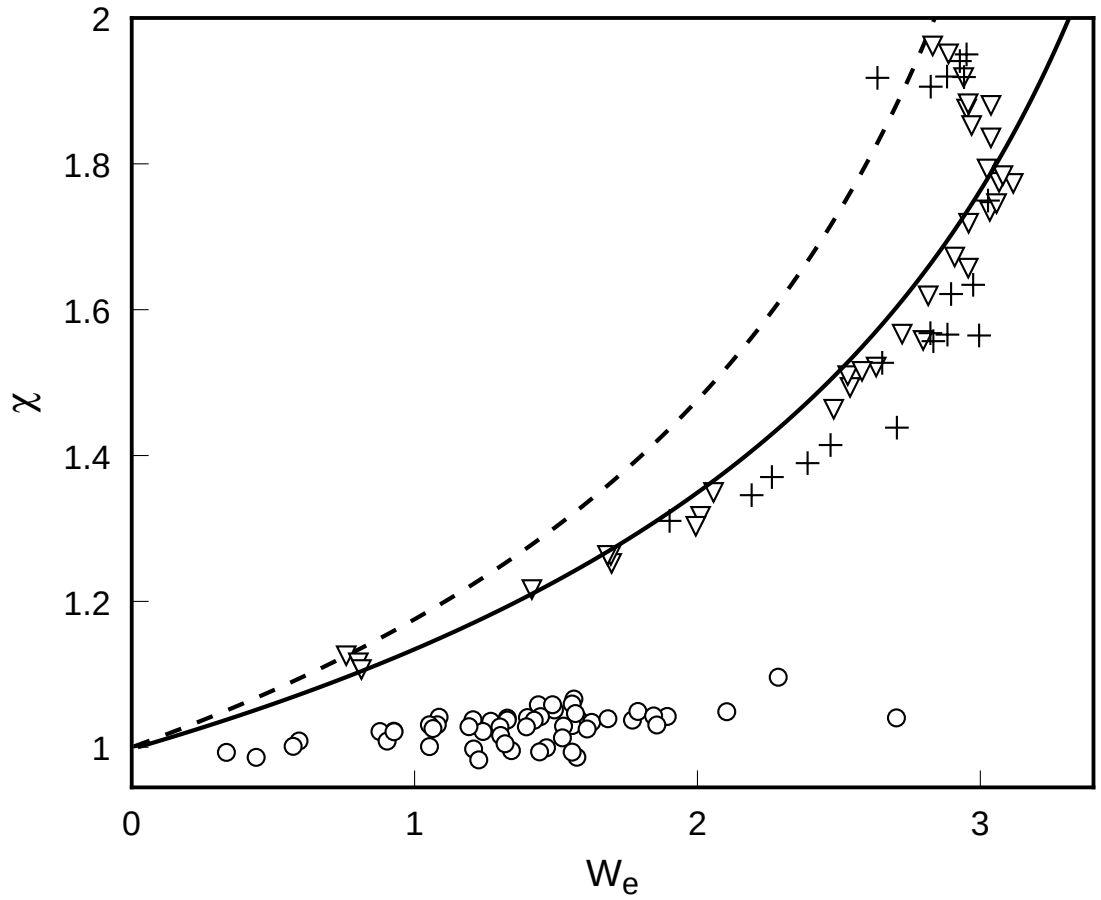

FIG. 3. Aspect ratio versus Weber number for bubbles generated by a gentle - push method with $d_i = 0.0267$ cm +, $d_i = 0.120$ cm ◯, and a pinch-off method ▽. Solid line is experimental results of Duineveld[4], dashed line is theoretical results of Moore[14].

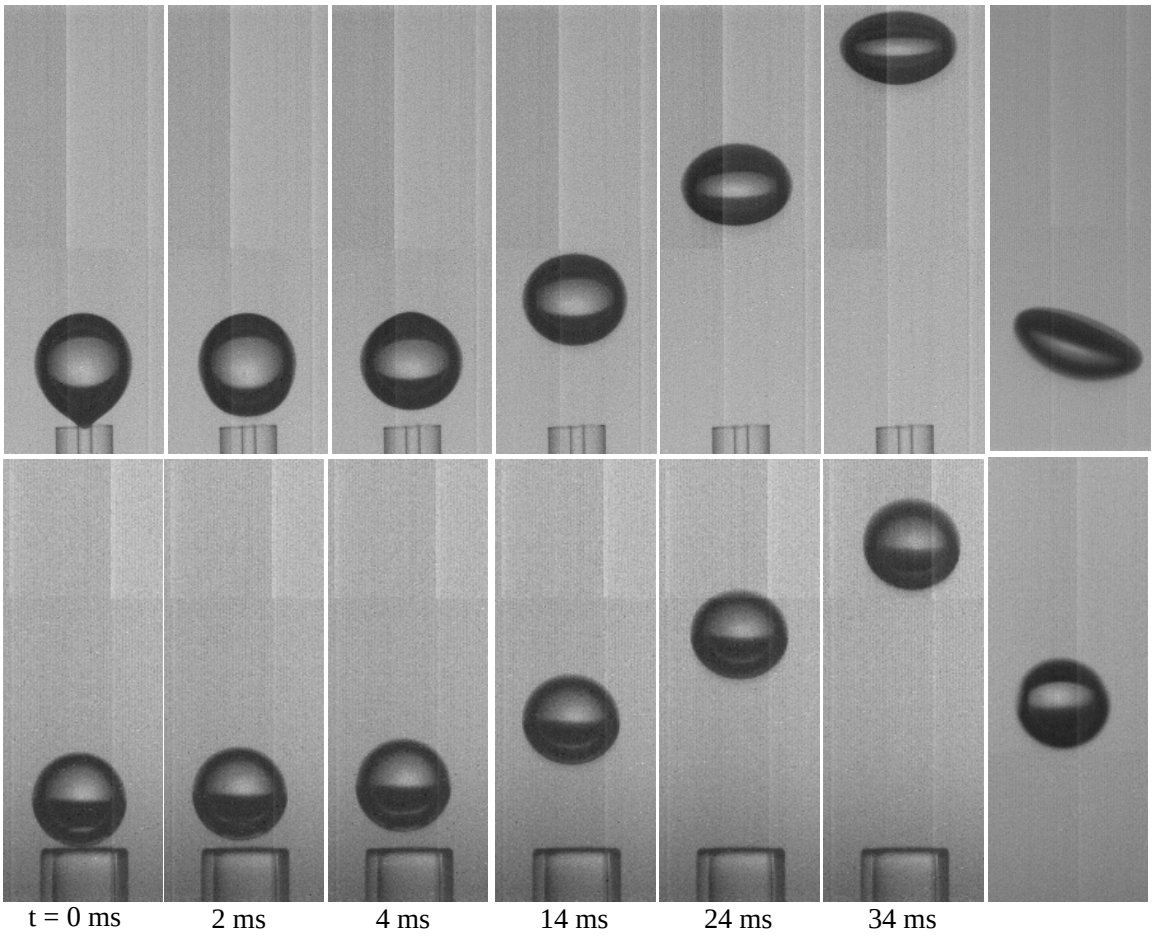

FIG. 4. Images of bubbles at detachment. The size of each image is 0.32 cm × 0.88 cm. In both cases, bubbles are generated by a gentle - push method. The capillary tube has an inner diameter of 0.0267 cm in the upper row and 0.120 cm in the lower row. The equivalent diameter of the bubble in the upper row is 0.195 cm, and lower row is 0.188 cm. The right most image in the upper(lower) row is taken at $\sim 6(20)cm$ above the capillary tip.

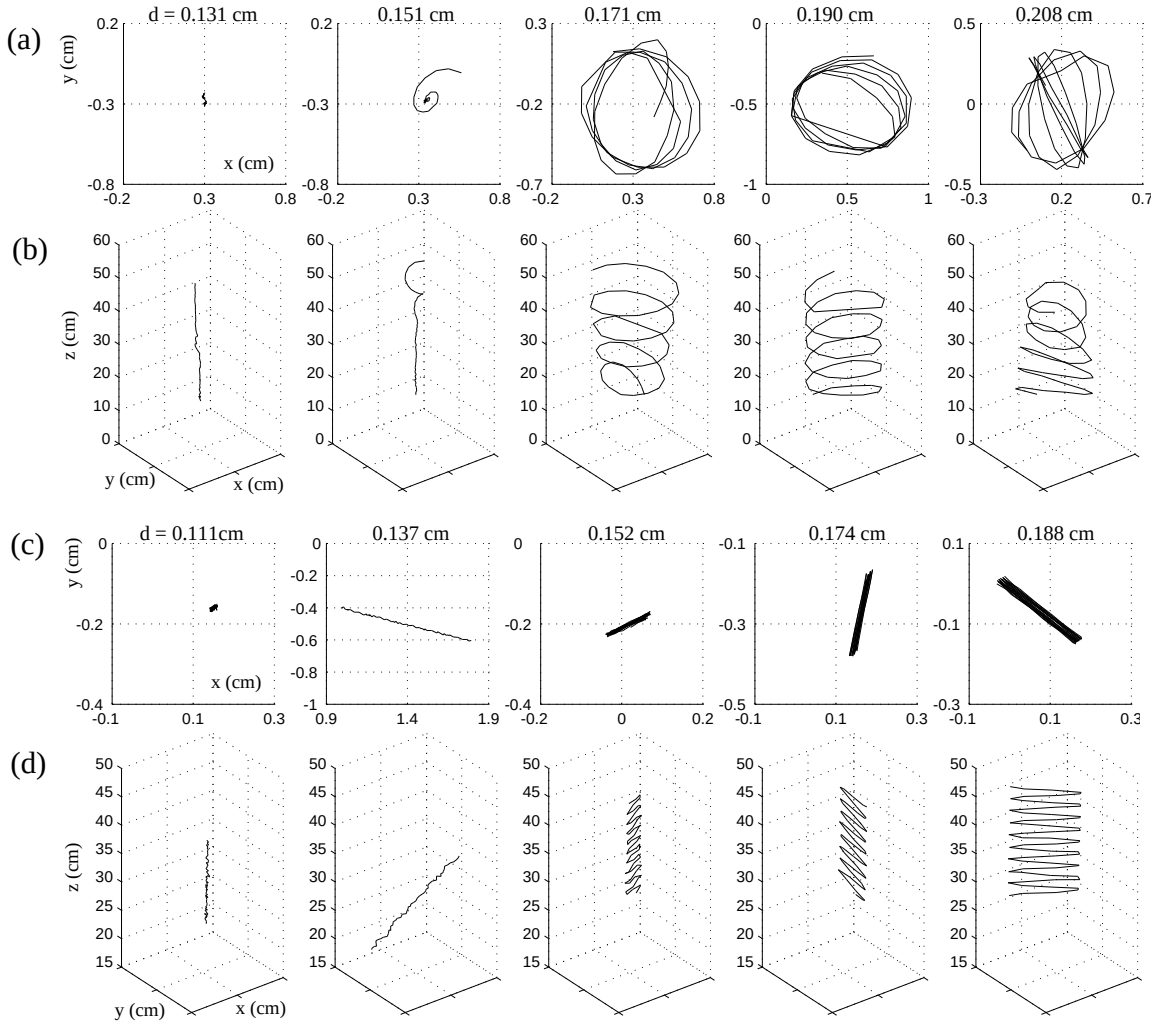

FIG. 5. a(c): Top view of the measured spiral(zigzag) trajectories. b(d): 3D rendition of the spiral(zigzag) trajectories. The diameter of the bubble d is labeled on each 2D trajectory plot.

REFERENCES

[1] R. Clift, J. R. Grace and M. E. Weber, *Bubbles, Drops and Particles*, (Academic, 1978).

[2] J. Magnaudet, I. Eames, "The motion of high-Reynolds-number bubbles in inhomogeneous flows," Annu. Rev. Fluid Mech., **32**, 659(2000).

[3] G. K. Batchelor, *An Introduction to Fluid Dynamics*, (Cambridge University Press, Cambridge, 1967).

[4] P. C. Duineveld, "The rise velocity and shape of bubbles in pure water at high Reynolds number," J. Fluid Mech. **292**, 325(1995).

[5] O. Miyagi, " The motion of air bubbles rising in water," Technol. Rep. Tohoku Univ. **5**, 135(1925).

[6] W. L. Haberman and R. K. Morton, "An experimental investigation of the drag and shape of air bubbles rising in various fluids," David Taylor Model Basin Report 802, 1953.

[7] P. G. Saffman, "On the rise of small air bubbles in water," J. Fluid Mech. **1**, 249 (1956).

[8] R. A. Hartunian and W. R. Sears, "On the instability of small gas bubbles moving uniformly in various liquids", J. Fluid Mech. **3**, 27 (1957).

[9] N. M. Aybers and A. Tapucu, " The motion of gas bubbles rising through stagnant liquid," Warme- und Stoffubertragung Bd. 2, 118(1969).

[10] T. Maxworthy, C. Gnann, M. Kürten and F. Durst, "Experiments on the rise of air bubbles in clean viscous liquids," J. Fluid Mech. **321**, 421 (1996).

[11] R. Bel Fdhila, P. C. Duineveld, "The effect of surfactant on the rise of a spherical bubble at high Reynolds and Peclet numbers," Phys. of Fluids **8**, 310(1996).

[12] C. E. Willert and M. Gharib, "Three-dimensional particle imaging with a single camera," Experiments in Fluids **12**, 353 (1992).

[13] The Culligan water purification system consists of one carbon filter, two 0.45μm filters, one reverse osmosis system, two deionization columns, one UV water sterilizer and two 0.22 μm filters. The specific resistance of the water is 10 MΩ·cm.

[14] D. W. Moore, "The velocity of rise of distorted gas bubbles in a liquid of small viscosity," J. Fluid Mech. **23**, 749(1965).

[15] K. Lunde and R. J. Perkins, "Observations on wakes behind spheroidal bubbles and particles," Paper number FEDSM97-3530, ASME-FED Summer Meeting, Vancouver, Canada , 1997.

[16] P. C. Duineveld, private communication, 2000.

[17] C. H. K. Williamson, Private communication, 2000.